The Physics of Galaxy Clusters

Christoph Pfrommer

Leibniz Institute for Astrophysics, Potsdam (AIP)

University of Potsdam

Lectures in the International Astrophysics Masters Program at Potsdam University

There are two basic approaches when teaching an astrophysical subject:

- present the subject historically
- explain the physics in a pedagogical order

There are two basic approaches when teaching an astrophysical subject:

- present the subject historically
- explain the physics in a pedagogical order

Outline of the tutorial:

- putting galaxy clusters into historical context
- going beyond clusters: the existence of superclusters
- putting the lectures into context
- answering your questions in the order of the lectures
- visual impressions: from images to astrophysics

AIP

Historical context of galaxy clusters – 1

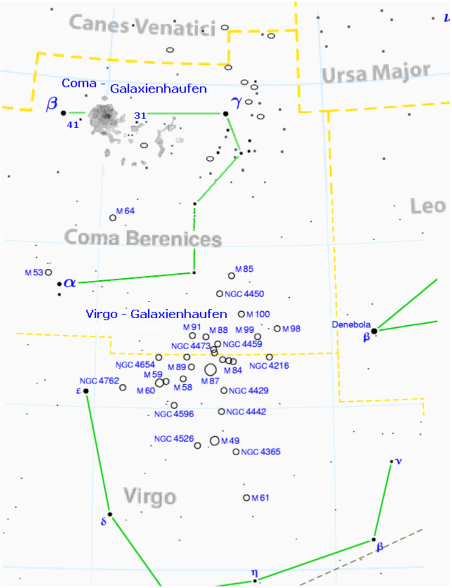

after Max Wolf 1901

Optical window:

- 1781: Charles Messier finds clustering of 16 objects (nebulae) towards the constellation Virgo

Historical context of galaxy clusters – 2

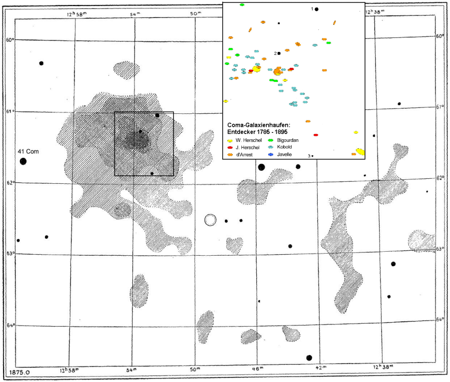

after Max Wolf 1901

Optical window:

- 1781: Charles Messier finds clustering of 16 objects (nebulae) towards the constellation Virgo
- 1783–1785: William Herschel discovers 23 objects (nebulae) that cluster towards the constellation Coma Berenice, but discovery controversial

Historical context of galaxy clusters – 2

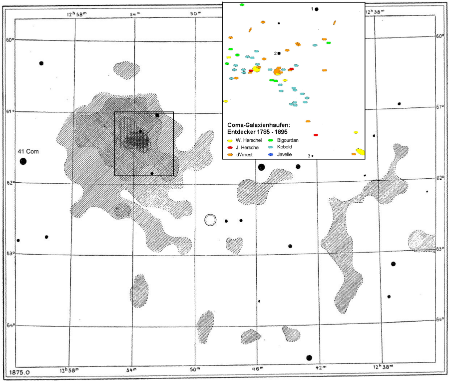

after Max Wolf 1901

Optical window:

- 1781: Charles Messier finds clustering of 16 objects (nebulae) towards the constellation Virgo
- 1783–1785: William Herschel discovers 23 objects (nebulae) that cluster towards the constellation Coma Berenice, but discovery controversial
- 1861–1867: Heinrich Ludwig d'Arrest confirms clustering of Coma galaxies

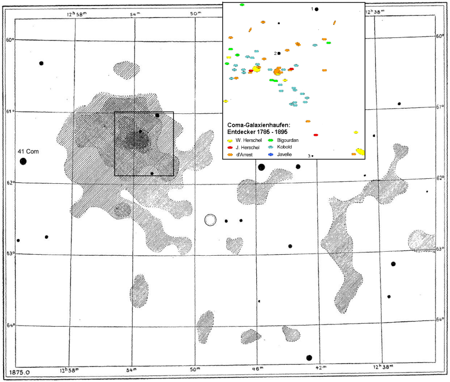

after Max Wolf 1901

Optical window:

- 1781: Charles Messier finds clustering of 16 objects (nebulae) towards the constellation Virgo
- 1783–1785: William Herschel discovers 23 objects (nebulae) that cluster towards the constellation Coma Berenice, but discovery controversial
- 1861–1867: Heinrich Ludwig d'Arrest confirms clustering of Coma galaxies
- In 1933, Fritz Zwicky pointed out that the Coma cluster must contain a substantial amount of dark matter to explain the large velocity dispersion of its galaxies

AIP

Historical context of galaxy clusters – 3

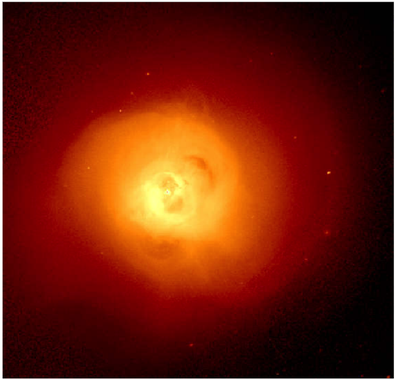
NASA/Chandra

- 1970s: X-ray observations find that galaxy clusters are among the brightest X-ray sources
- improved angular resolution: the entire galaxy cluster glows in X-rays, filling in the volume in between the galaxies

X-rays are generated via

1. bremsstrahlung emission of hot thermal electrons, and
2. line emission from recombination of atoms.

AIP

Historical context of galaxy clusters – 4

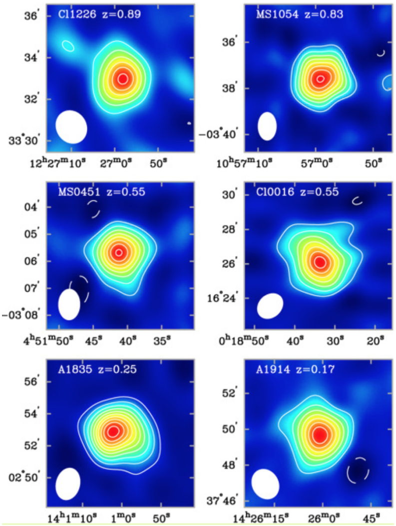

Joy+ (2001)

- 1972: Sunyaev & Zel'dovich propose CMB observations towards galaxy clusters to elucidate the nature of cluster X-ray radiation
- CMB decrement at $\nu < 217$ GHz argues for bremsstrahlung X-ray emission from a hot thermal plasma

Historical context of galaxy clusters – 4

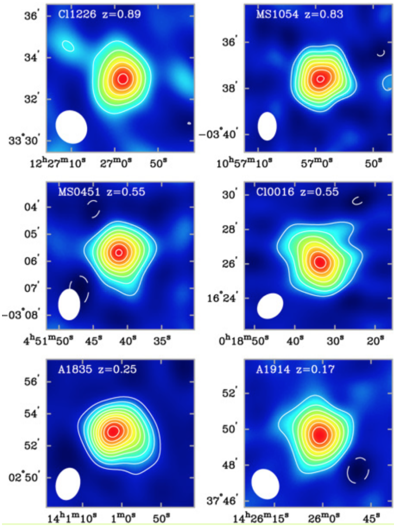

Joy+ (2001)

- 1972: Sunyaev & Zel'dovich propose CMB observations towards galaxy clusters to elucidate the nature of cluster X-ray radiation
- CMB decrement at $\nu < 217$ GHz argues for bremsstrahlung X-ray emission from a hot thermal plasma
- late 1990s: interferometric CMB observations detected the SZ effect
- CMB surveys used to find clusters because the SZ effect is independent of redshift

AIP

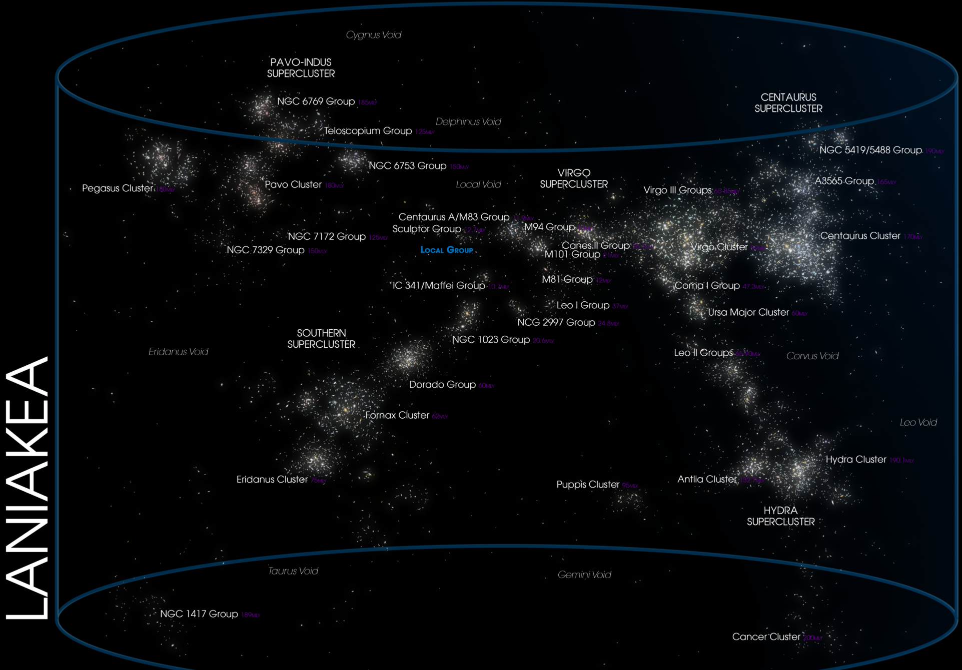

The Laniakea Supercluster (Colvin 2018)

The Laniakea Supercluster – 1

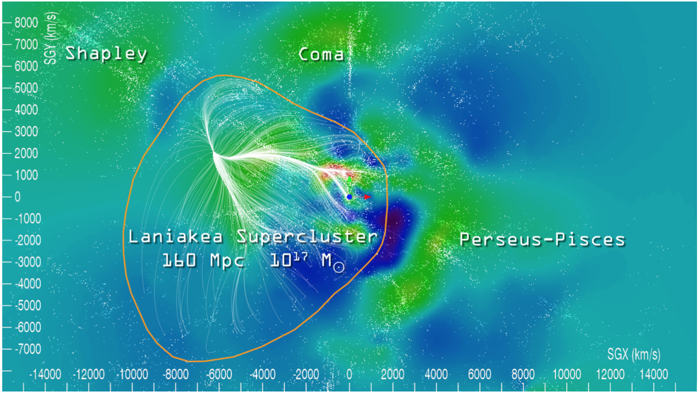

Tully+ (2014)

- A slice of the Laniakea Supercluster in the supergalactic equatorial plane with individual galaxies (white dots).
- Colours represent density values within the equatorial slice: red at high densities and blue in voids.
- Velocity flow streams within the Laniakea basin of attraction are shown in white. The orange contour encloses the outer limits of these streams.

AIP

The Laniakea Supercluster – 2

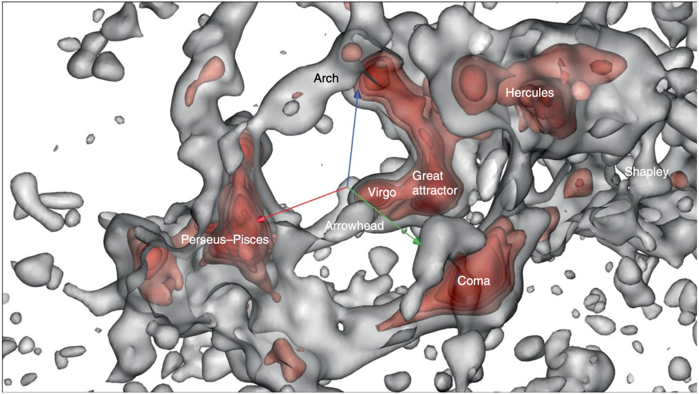

Hoffman+ (2018)

- "Quasi-linear" map of the local universe, with the Earth at the centre of the three arrows.
- The main superclusters are shown deep inside dense (red) regions.

- ***Overview and background:***

- ***Evolution of the dark component***

- ***Evolution of the baryonic component***

- ***Overview and background:***
  - What is a galaxy cluster? Insights from observations at various wavelengths
  - Why are clusters interesting? Tools for cosmology and laboratories for high-energy and plasma astrophysics
- ***Evolution of the dark component***
  - When do clusters form? $\Rightarrow$ statistics and power spectra
  - Where do cluster form? $\Rightarrow$ non-linear evolution
  - How do clusters form? $\Rightarrow$ spherical collapse model
  - How many clusters are there? $\Rightarrow$ Press-Schechter mass function
  - What is the structure of a cluster? $\Rightarrow$ halo density profiles, virial masses
- ***Evolution of the baryonic component***
  - Non-radiative physics
  - Radiative physics
  - Non-thermal processes

AIP

- ***Evolution of the baryonic component***
  - *Non-radiative physics*
  - *Radiative physics*
  - *Non-thermal processes*

- ***Evolution of the baryonic component***
  - *Non-radiative physics*
    - Adiabatic Processes and Entropy
    - Basic Conservation Equations
    - Buoyancy Instabilities
    - Vorticity and Turbulence
    - Shocks and jump conditions
    - Entropy generation by accretion and hierarchical merging
    - Scaling relations (ideal and real)
  - *Radiative physics*
    - Radiative cooling and star formation
    - Energy feedback (supernovae, active galactic nuclei)
    - Transport processes of gas: conduction, thermal stability (without and with magnetic fields)
  - *Non-thermal processes*
    - Origin and transport of magnetic fields, magneto-hydrodynamic turbulence
    - Acceleration of cosmic rays (to first and second order), transport equation

- ***Cluster physics informed by different observables:***
  - *Optical: galaxy properties and virial theorem*
  - *Gravitational lensing*
  - *X-rays: gastrophysics at high-resolution*
  - *Sunyaev-Zel'dovich effect: the thermal energy content*
  - *Radio halos and relics: watching powerful shocks and plasma physics at work*

- ***Cluster physics informed by different observables:***
  - *Optical: galaxy properties and virial theorem*
    - Transforming galaxy populations: ram pressure, tidal effects, dynamical friction
    - Weighting clusters (1): virial theorem
  - *Gravitational lensing*
    - Deflection angle, lens equation, Einstein radius, lensing potential
    - Weighting clusters (2): strong and weak cluster lensing
  - *X-rays: gastrophysics at high-resolution*
    - Weighting clusters (3): hydrostatic equilibrium masses
    - Kinematics of shocks and cold fronts
    - Probing kinetic equilibrium with collisionless shocks
    - Width of cold fronts - magnetic draping
  - *Sunyaev-Zel'dovich effect: the thermal energy content*
    - Thermal and kinetic SZ effect
    - Properties and SZ scaling relation, SZ power spectrum
  - *Radio halos and relics: watching powerful shocks and plasma physics at work*

Cluster mergers: *the* most energetic cosmic events

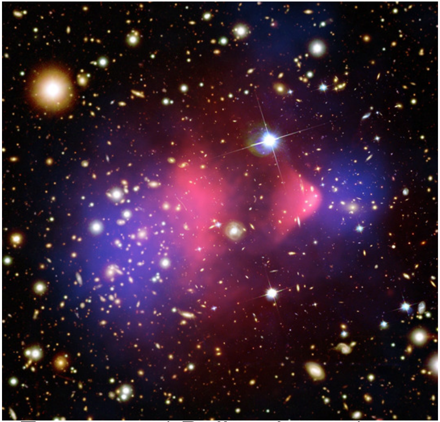

1E 0657-56 (“Bullet cluster”)

(X-ray: NASA/CXC/CfA/M.Markevitch et al.; Optical: NASA/STScI; Magellan/U.Arizona/D.Clowe et al.; Lensing: NASA/STScI; ESO WFI; Magellan/U.Arizona/D.Clowe et al.)

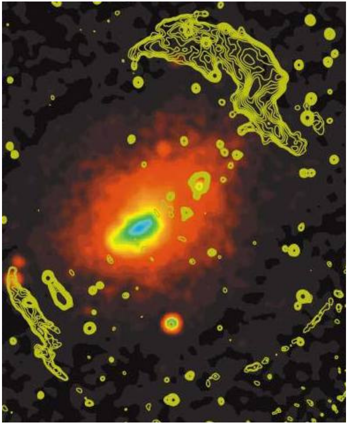

Abell 3667

(radio: Johnston-Hollitt. X-ray: ROSAT/PSPC.)

AIP

The structure of our Universe

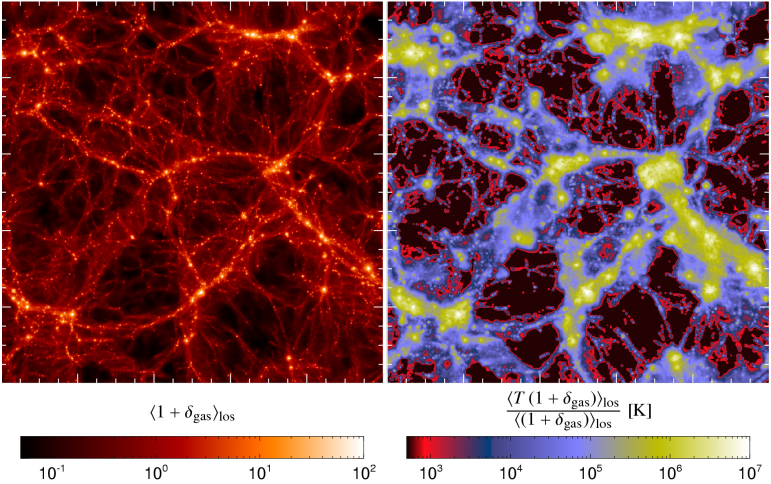

The "cosmic web" today. *Left:* the projected gas density in a cosmological simulation. *Right:* gravitationally heated intergalactic medium (C.P. et al. 2006).

Cosmological cluster simulation: gas density

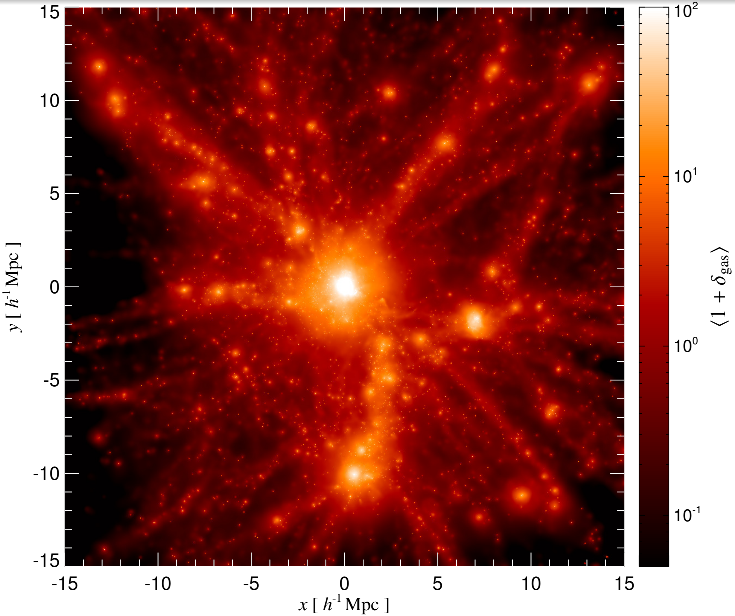

AIP

Mass weighted temperature

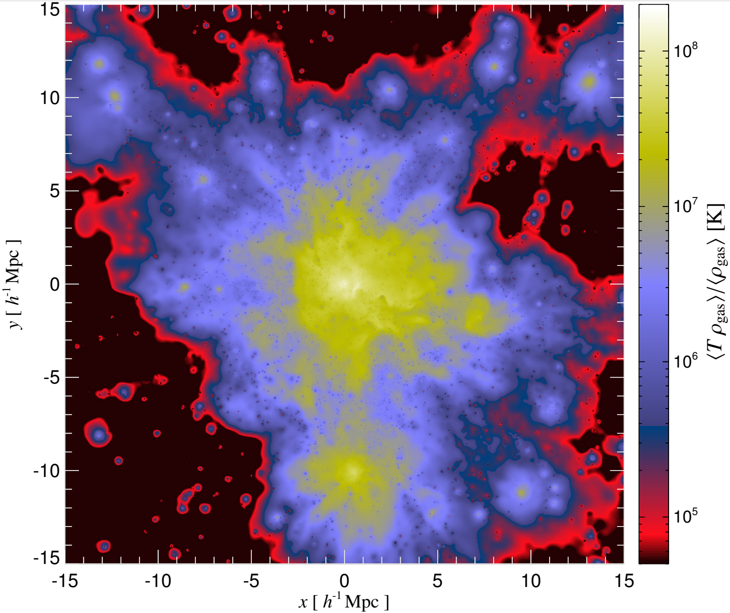

AIP

Shock strengths weighted by dissipated energy

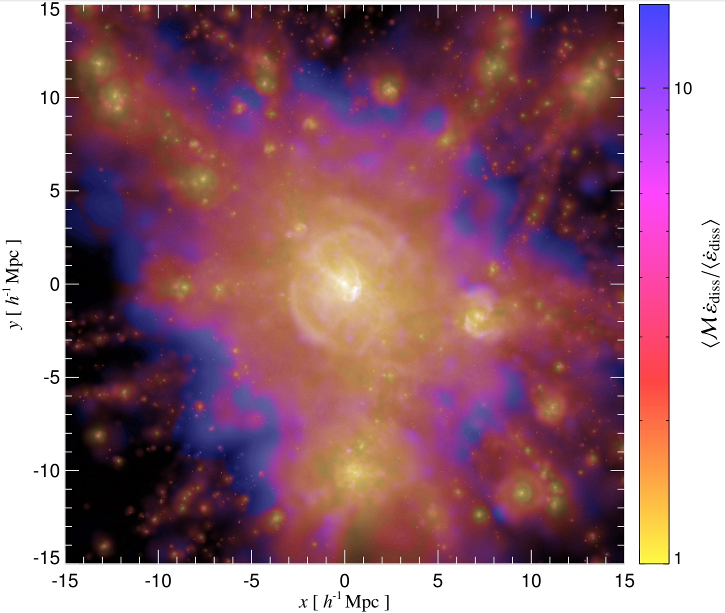

Sunyaev-Zel'dovich effect: integrated thermal pressure

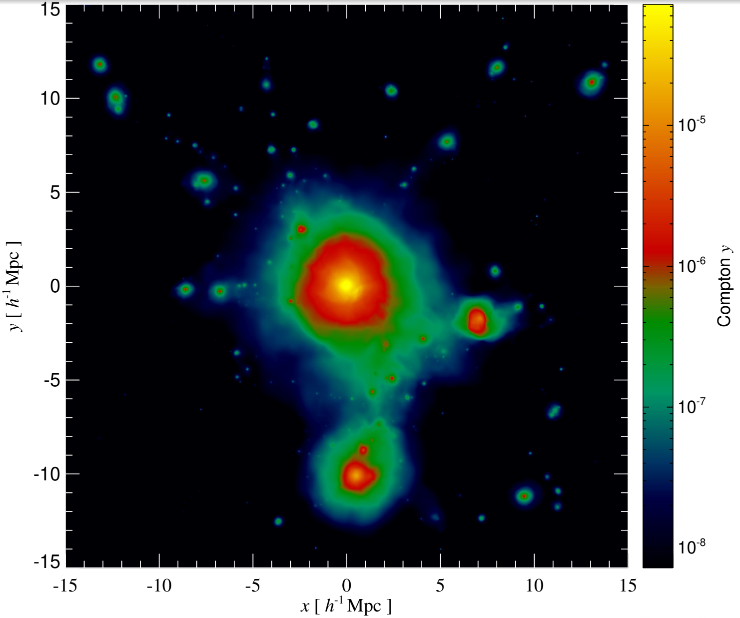

Thermal X-ray emission: gas density squared

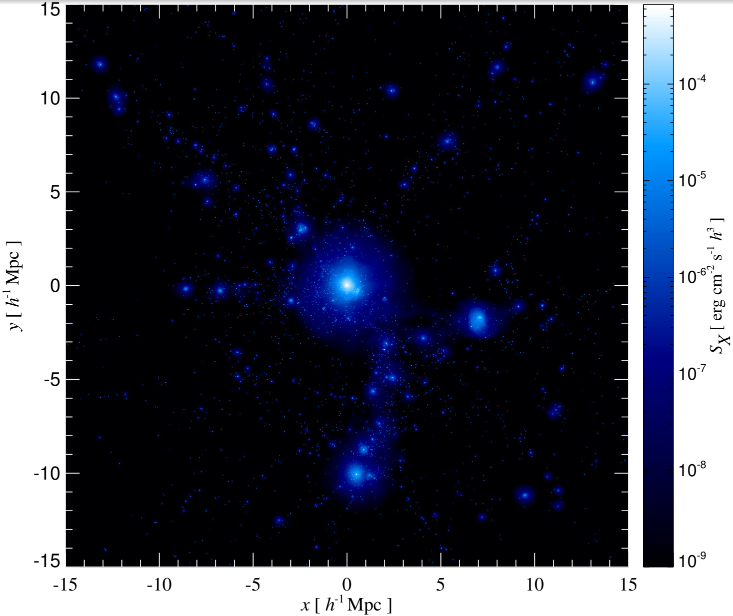

AIP

Zooming on the cluster: thermal cluster gas

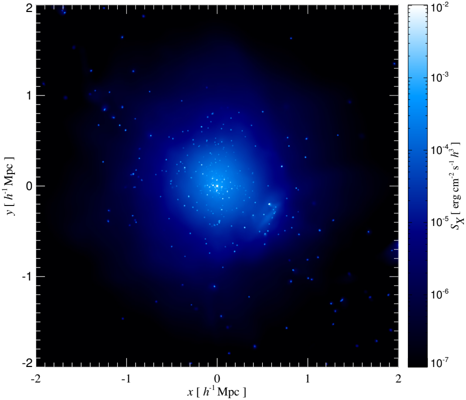

Thermal bremsstrahlung emission,

merging cluster, $M_{\rm vir} \simeq 10^{15} M_\odot / h$

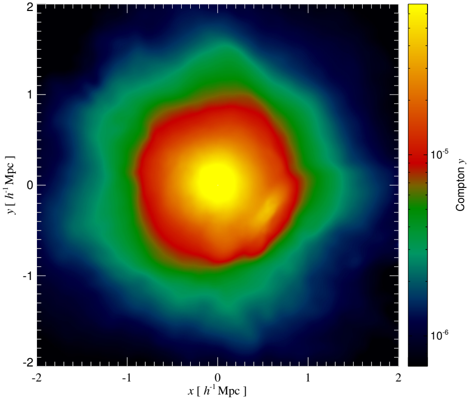

Sunyaev-Zel'dovich effect,

merging cluster, $M_{\rm vir} \simeq 10^{15} M_\odot / h$

Zooming on the cluster: optical vs. radio synchrotron

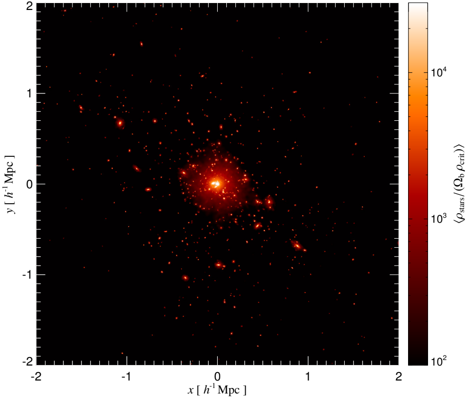

Stellar mass density ("cluster galaxies"),

merging cluster, $M_{\mathrm{vir}} \simeq 10^{15} M_{\odot}/h$

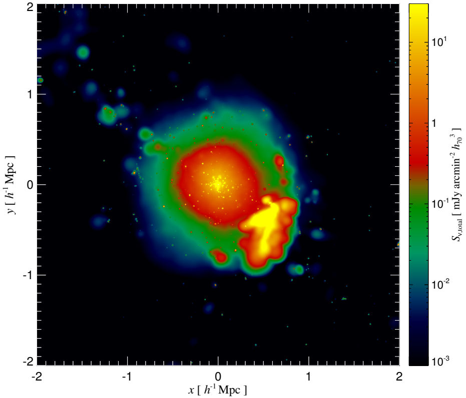

Radio halo and relic emission,

merging cluster, $M_{\mathrm{vir}} \simeq 10^{15} M_{\odot}/h$

Questions – Sunyaev Zel'dovich effect

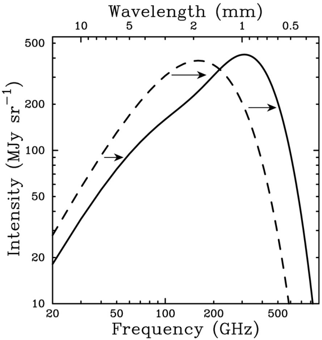

- Why does the SZ distortion crosses over at 217 GHz?

Questions – Sunyaev Zel'dovich effect

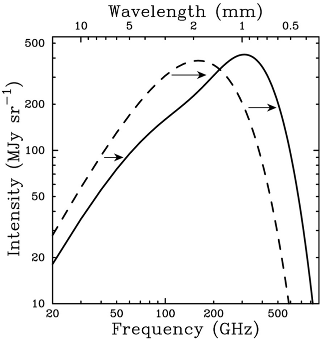

- Why does the SZ distortion crosses over at 217 GHz? $\Rightarrow$ solution of the Kompaneet's equation, but kinetic and relativistic SZ effect moves the null

Questions – Sunyaev Zel'dovich effect

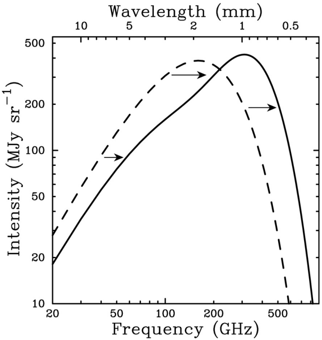

- Why does the SZ distortion crosses over at 217 GHz? $\Rightarrow$ solution of the Kompaneet's equation, but kinetic and relativistic SZ effect moves the null

- If only 1 photon out of every 2000 experiences a scattering then how is that we can observe this effect in the first place?

Questions – Sunyaev Zel'dovich effect

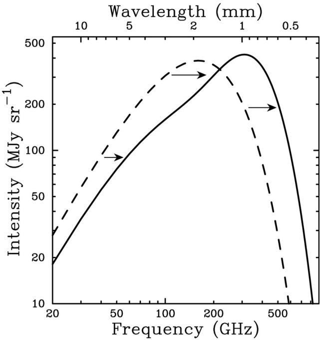

- Why does the SZ distortion crosses over at 217 GHz?
  $\Rightarrow$ solution of the Kompaneet's equation, but kinetic and relativistic SZ effect moves the null

- If only 1 photon out of every 2000 experiences a scattering then how is that we can observe this effect in the first place?
  $\Rightarrow$ we need to observe many photons: interferometric CMB observations are great for tiny differences in surface brightness

Questions – Sunyaev Zel'dovich effect

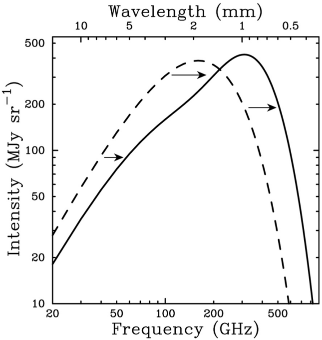

- Why does the SZ distortion crosses over at 217 GHz?
  $\Rightarrow$ solution of the Kompaneet's equation, but kinetic and relativistic SZ effect moves the null

- If only 1 photon out of every 2000 experiences a scattering then how is that we can observe this effect in the first place?
  $\Rightarrow$ we need to observe many photons: interferometric CMB observations are great for tiny differences in surface brightness
- In the derivation of the Compton y parameter we have neglected the redshift range from 9 to 1100, why?

Questions – Sunyaev Zel'dovich effect

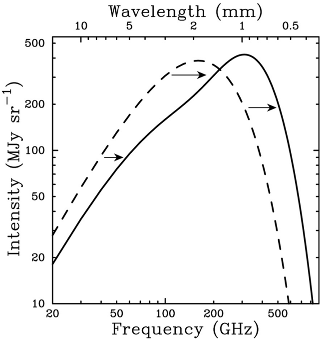

- Why does the SZ distortion crosses over at 217 GHz?
  $\Rightarrow$ solution of the Kompaneet's equation, but kinetic and relativistic SZ effect moves the null

- If only 1 photon out of every 2000 experiences a scattering then how is that we can observe this effect in the first place?
  $\Rightarrow$ we need to observe many photons: interferometric CMB observations are great for tiny differences in surface brightness
- In the derivation of the Compton y parameter we have neglected the redshift range from 9 to 1100, why?
  $\Rightarrow$ because the SZ effect describes photon-electron scattering and the universe is becoming neutral at around $z \sim 1100$ and get reionized at $z \sim 9$: so there are no free electrons around at these high redshifts

AIP

The matter power spectrum

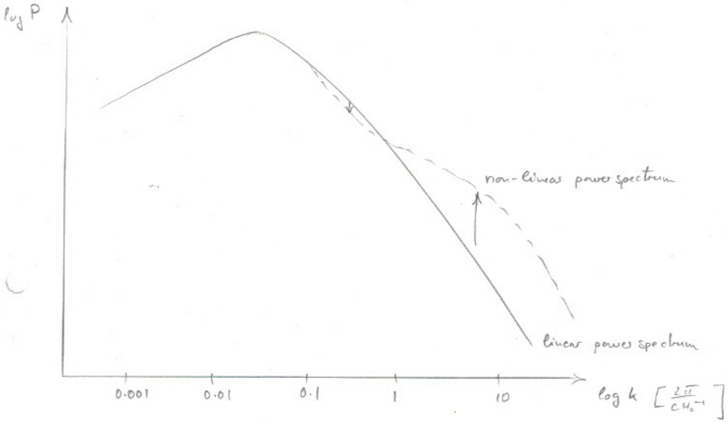

- non-linear structure formation causes more strongly enhanced density fluctuations on small scales
- development of a bump at large wave vectors (small spatial scales) in the non-linear matter power spectrum at the expense of intermediate scales

The scaled matter power spectrum

Variance of the matter density fluctuations as a function of wave number, $\sigma^2(k)$

- For a cold dark matter (CDM) cosmology, the linear power spectrum of matter density fluctuations δ reads

$$P(k) \propto \begin{cases} k & (k < k_0) \\ k^{-3} & (k \gg k_0). \end{cases}$$

Here, $k_0 = 2\pi a_{\mathrm{eq}}/\lambda_0$ is the comoving wave number of the particle horizon at matter-radiation equality.

The scaled matter power spectrum

Variance of the matter density fluctuations as a function of wave number, $\sigma^2(k)$

- For a cold dark matter (CDM) cosmology, the linear power spectrum of matter density fluctuations δ reads

$$P(k) \propto \begin{cases} k & (k < k_0) \\ k^{-3} & (k \gg k_0). \end{cases}$$

  Here, $k_0 = 2\pi a_{\mathrm{eq}}/\lambda_0$ is the comoving wave number of the particle horizon at matter-radiation equality.

- The variance of δ is the correlation function at $y = 0$ (Eq. 2.30 in the notes), which is the k space integrated power spectrum

$$\sigma^2 = 4\pi \int \frac{k^2 \mathrm{d}k}{(2\pi)^3} P(k) \, .$$

The scaled matter power spectrum

Variance of the matter density fluctuations as a function of wave number, $\sigma^2(k)$

- For a cold dark matter (CDM) cosmology, the linear power spectrum of matter density fluctuations δ reads

$$P(k) \propto \begin{cases} k & (k < k_0) \\ k^{-3} & (k \gg k_0). \end{cases}$$

  Here, $k_0 = 2\pi a_{\mathrm{eq}}/\lambda_0$ is the comoving wave number of the particle horizon at matter-radiation equality.

- The variance of δ is the correlation function at $y = 0$ (Eq. 2.30 in the notes), which is the k space integrated power spectrum

$$\sigma^2 = 4\pi \int \frac{k^2 \mathrm{d}k}{(2\pi)^3} P(k) \,.$$

- Hence, to order of magnitude, we obtain

$$\sigma^2 \sim k^3 P(k) \,.$$

Hierarchical formation: when do clusters form?

Variance of the matter density fluctuations as a function of wave number, $\sigma^2(k)$

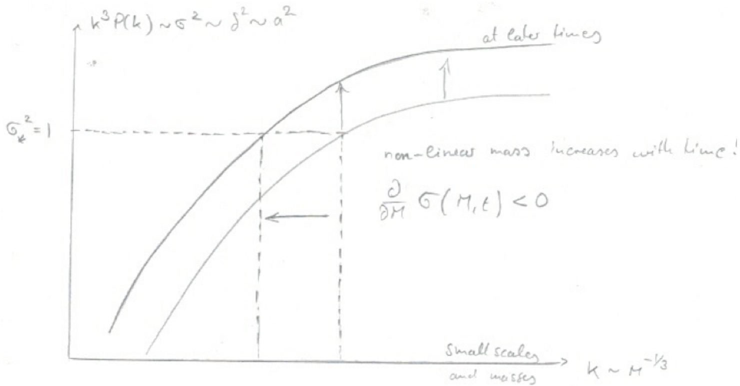

Hierarchical formation: when do clusters form?

Variance of the matter density fluctuations as a function of wave number, $\sigma^2(k)$

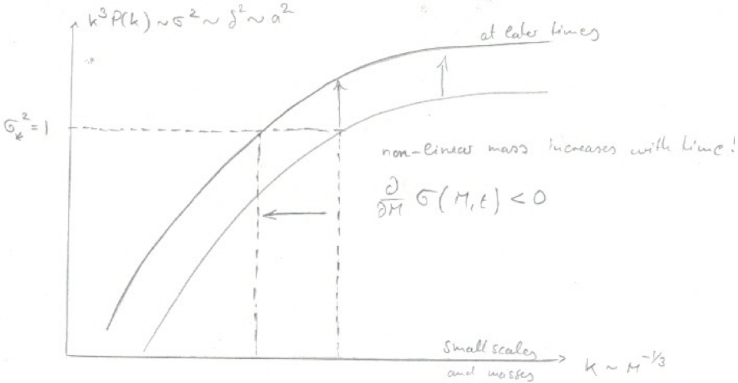

- more power on small scales, which first go non-linear ($\sigma^2 > 1$) and thus collapse first: dwarf galaxies form before large galaxies, which form before galaxy clusters

Hierarchical formation: when do clusters form?

Variance of the matter density fluctuations as a function of wave number, $\sigma^2(k)$

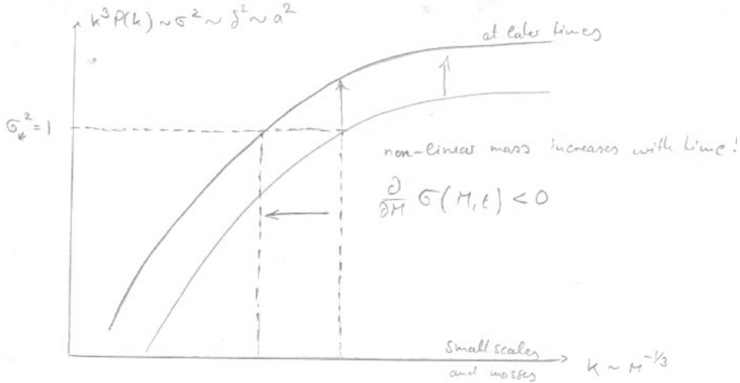

- more power on small scales, which first go non-linear ($\sigma^2 > 1$) and thus collapse first: dwarf galaxies form before large galaxies, which form before galaxy clusters
- critical wave number at which the fluctuation strength becomes non-linear decreases with time (spatial scale increases with time)

Hierarchical formation: when do clusters form?

Variance of the matter density fluctuations as a function of wave number, $\sigma^2(k)$

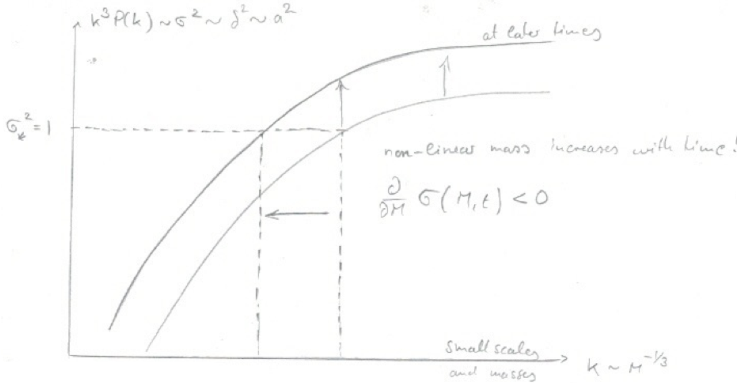

- more power on small scales, which first go non-linear ($\sigma^2 > 1$) and thus collapse first: dwarf galaxies form before large galaxies, which form before galaxy clusters
- critical wave number at which the fluctuation strength becomes non-linear decreases with time (spatial scale increases with time)
- structure forms "bottom-up" in ΛCDM cosmologies: hence we speak about hierarchical galaxy formation

Hierarchical formation: when do clusters form?

Variance of the matter density fluctuations as a function of collapsed mass, $\sigma^2(M)$

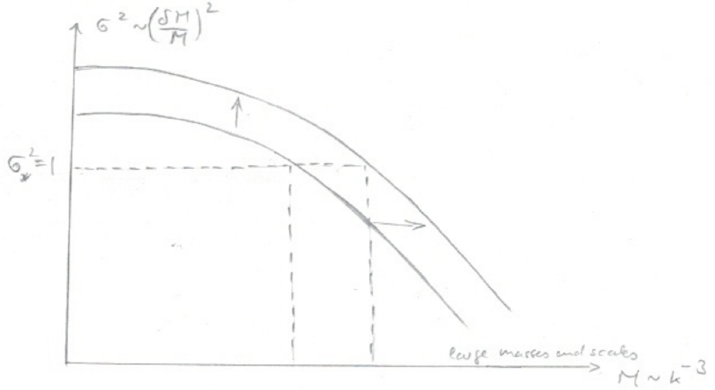

- more power on small scales, which first go non-linear ($\sigma^2 > 1$) and thus collapse first: dwarf galaxies form before large galaxies, which form before galaxy clusters
- critical wave number at which the fluctuation strength becomes non-linear decreases with time (spatial scale increases with time)
- structure forms "bottom-up" in ΛCDM cosmologies: hence we speak about hierarchical galaxy formation

AIP

The initial power spectrum

Potential fluctuations make case for Harrison-Zel'dovich-Peebles spectrum

- Let's look at the fluctuations in the gravitational potential (at fixed volume),

$$\delta\Phi \sim \frac{GM}{R}\frac{\delta M}{M} \sim GM^{2/3}\bar{\rho}^{1/3}\frac{\delta M}{M}$$

  since at any time $R \propto (M/\bar{\rho})^{1/3}$.
- Unless $\delta M/M \propto M^{-2/3}$, the potential fluctuations $\delta\Phi$ will diverge. Depending on the power-law index of $\delta M/M \propto M^{-\alpha}$, $\delta\Phi$ will diverge on large scales or masses (for $\alpha < 2/3$) or on small scales or masses (for $\alpha > 2/3$).

AIP

The initial power spectrum

Potential fluctuations make case for Harrison-Zel'dovich-Peebles spectrum

- Let's look at the fluctuations in the gravitational potential (at fixed volume),

$$\delta\Phi \sim \frac{GM}{R}\frac{\delta M}{M} \sim GM^{2/3}\bar{\rho}^{1/3}\frac{\delta M}{M}$$

  since at any time $R \propto (M/\bar{\rho})^{1/3}$.
- Unless $\delta M/M \propto M^{-2/3}$, the potential fluctuations $\delta\Phi$ will diverge. Depending on the power-law index of $\delta M/M \propto M^{-\alpha}$, $\delta\Phi$ will diverge on large scales or masses (for $\alpha < 2/3$) or on small scales or masses (for $\alpha > 2/3$).
- For large masses, we have

$$\delta\Phi \propto M^{2/3-\alpha} \overset{M\to\infty}{\Longrightarrow} \infty \quad \text{for } \alpha < 2/3.$$

The initial power spectrum

Potential fluctuations make case for Harrison-Zel'dovich-Peebles spectrum

- Let's look at the fluctuations in the gravitational potential (at fixed volume),

$$\delta\Phi \sim \frac{GM}{R}\frac{\delta M}{M} \sim GM^{2/3}\bar{\rho}^{1/3}\frac{\delta M}{M}$$

since at any time $R \propto (M/\bar{\rho})^{1/3}$.

- Unless $\delta M/M \propto M^{-2/3}$, the potential fluctuations $\delta\Phi$ will diverge. Depending on the power-law index of $\delta M/M \propto M^{-\alpha}$, $\delta\Phi$ will diverge on large scales or masses (for $\alpha < 2/3$) or on small scales or masses (for $\alpha > 2/3$).
- For large masses, we have

$$\delta\Phi \propto M^{2/3-\alpha} \overset{M\to\infty}{\Longrightarrow} \infty \quad \text{for } \alpha < 2/3.$$

- On small scales or masses (large k values), we have $M \propto R^3 \propto k^{-3}$ so that

$$\frac{\delta M}{M} \propto \frac{\delta k}{k} \propto k^{3\alpha}.$$

Hence, the potential fluctuations $\delta\Phi$ also diverge on small scales

$$\delta\Phi \propto M^{2/3-\alpha} \propto k^{-2+3\alpha} = k^{3(\alpha-2/3)} \overset{k\to\infty}{\Longrightarrow} \infty \quad \text{for } \alpha > 2/3.$$

AIP

Spherical collapse: solution

- What is the difference between the calculation of virialized density contrast at collapse vs. the linear counterpart?

Spherical collapse: solution

- What is the difference between the calculation of virialized density contrast at collapse vs. the linear counterpart?
- The spherical collapse problem has the following parametric solution, which describes a cycloid,

$$
\begin{aligned}
R &= A(1-\cos\theta)\,, \quad A = \frac{GM}{2|\Phi|}\,, \\
t &= B(\theta-\sin\theta)\,, \quad B = \frac{GM}{(2|\Phi|)^{3/2}}\,.
\end{aligned}
$$

Spherical collapse: solution

- What is the difference between the calculation of virialized density contrast at collapse vs. the linear counterpart?
- The spherical collapse problem has the following parametric solution, which describes a cycloid,

$$\begin{aligned} R &= A(1-\cos\theta)\,, \quad A = \frac{GM}{2|\Phi|}\,, \\ t &= B(\theta-\sin\theta)\,, \quad B = \frac{GM}{(2|\Phi|)^{3/2}}\,. \end{aligned}$$

- The mean density inside the sphere is

$$\rho = \frac{M}{4\pi/3\,R^3} = \frac{3M}{4\pi A^3}\frac{1}{(1-\cos\theta)^3}\,,$$

while the mean density of the background universe with $\Omega_{\mathrm{m0}} = 1$ is

$$\bar\rho = \frac{3H^2}{8\pi G} = \frac{1}{6\pi G t^2} = \frac{1}{6\pi G B^2}\frac{1}{(\theta-\sin\theta)^2}\,,$$

with $H = 2/(3t)$. The overdensity of the sphere (which is generally non-linear) can be obtained by combining these equations to yield

$$1+\delta = \frac{\rho}{\bar\rho} = \frac{9}{2}\frac{(\theta-\sin\theta)^2}{(1-\cos\theta)^3}\,. \tag{1}$$

Spherical collapse: characteristic overdensities

- We find different values for the density contrast at collapse ($t = t_c = 2t_{max}$) of

$$\delta_c \equiv \delta_{lin}(t_c) = \frac{3}{20}(12\pi)^{2/3} \approx 1.686,$$
$$\delta_v \equiv \delta_{coll} = 18\pi^2 - 1 = 177\ .$$

Where and how are the two values used?

Spherical collapse: characteristic overdensities

- We find different values for the density contrast at collapse ($t = t_c = 2t_{max}$) of

$$\delta_c \equiv \delta_{lin}(t_c) = \frac{3}{20}(12\pi)^{2/3} \approx 1.686,$$
$$\delta_v \equiv \delta_{coll} = 18\pi^2 - 1 = 177\ .$$

  Where and how are the two values used?

- The first value (δ_c) was obtained by linearizing Eq. (1) and extrapolating the result to $t = t_c$. It can thus only be applied to the density fluctuations in the linear regime to extrapolate the fate of a given (filtered) overdensity, i.e., whether its mass is large enough to eventually collapse to a halo (Press-Schechter formalism).

AIP

Spherical collapse: characteristic overdensities

- We find different values for the density contrast at collapse ($t = t_c = 2t_{max}$) of

$$\delta_c \equiv \delta_{lin}(t_c) = \frac{3}{20}(12\pi)^{2/3} \approx 1.686,$$
$$\delta_v \equiv \delta_{coll} = 18\pi^2 - 1 = 177 \; .$$

Where and how are the two values used?

- The first value (δ_c) was obtained by linearizing Eq. (1) and extrapolating the result to $t = t_c$. It can thus only be applied to the density fluctuations in the linear regime to extrapolate the fate of a given (filtered) overdensity, i.e., whether its mass is large enough to eventually collapse to a halo (Press-Schechter formalism).
- The virialized density contrast δ_v looks at an actually collapsed and virialized halo for which we found $R_f = R_{ta}/2$. Hence, it is used to identify halos (in simulations, observations) via the definition of the halo mass

$$M_{\Delta,m}\left(\frac{4\pi}{3}r_\Delta^3\right)^{-1} = \Delta\bar{\rho}_m(a).$$

where $\Delta = 177$, 200, or 500, depending on the specific application.

- Sometimes, $\bar{\rho}_m(a)$ is exchanged for $\rho_{cr}(a)$

AIP

Spherical collapse: virialization

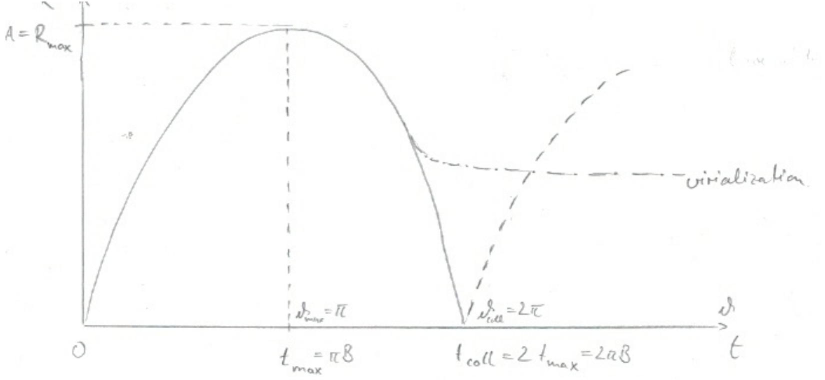

The derivation of the halo mass function

- We assumed a Gaussian distribution for the probability of finding a filtered density contrast $\bar{\delta}(\boldsymbol{x})$ at $\boldsymbol{x}$:

$$p(\bar{\delta}, a) = \frac{1}{\sqrt{2\pi\sigma_R^2(a)}} \exp\left[-\frac{\bar{\delta}^2(\boldsymbol{x})}{2\sigma_R^2(a)}\right] ,$$

where the variance σ_R depends on time.

AIP

The derivation of the halo mass function

- We assumed a Gaussian distribution for the probability of finding a filtered density contrast $\bar{\delta}(\boldsymbol{x})$ at $\boldsymbol{x}$:

$$p(\bar{\delta}, a) = \frac{1}{\sqrt{2\pi\sigma_R^2(a)}} \exp\left[-\frac{\bar{\delta}^2(\boldsymbol{x})}{2\sigma_R^2(a)}\right] ,$$

  where the variance σ_R depends on time.

- The probability of finding the filtered density contrast at or above the linear density contrast for spherical collapse, $\bar{\delta} > \delta_c$, is equal to the fraction of the cosmic volume filled with haloes of mass M,

$$F(M, a) = \int_{\delta_c}^{\infty} \mathrm{d}\bar{\delta}\, p(\bar{\delta}, a) = \int_{\delta_c}^{\infty} \mathrm{d}\bar{\delta} \frac{1}{\sqrt{2\pi\sigma_R^2(a)}} \exp\left[-\frac{\bar{\delta}^2(\boldsymbol{x})}{2\sigma_R^2(a)}\right]$$

The derivation of the halo mass function

- We assumed a Gaussian distribution for the probability of finding a filtered density contrast $\bar{\delta}(\boldsymbol{x})$ at $\boldsymbol{x}$:

$$p(\bar{\delta}, a) = \frac{1}{\sqrt{2\pi\sigma_R^2(a)}} \exp\left[-\frac{\bar{\delta}^2(\boldsymbol{x})}{2\sigma_R^2(a)}\right] ,$$

  where the variance σ_R depends on time.

- The probability of finding the filtered density contrast at or above the linear density contrast for spherical collapse, $\bar{\delta} > \delta_c$, is equal to the fraction of the cosmic volume filled with haloes of mass M,

$$F(M, a) = \int_{\delta_c}^{\infty} d\bar{\delta} p(\bar{\delta}, a) = \int_{\delta_c}^{\infty} d\bar{\delta} \frac{1}{\sqrt{2\pi\sigma_R^2(a)}} \exp\left[-\frac{\bar{\delta}^2(\boldsymbol{x})}{2\sigma_R^2(a)}\right]$$

- After substitution, we obtain

$$F(M, a) = \frac{1}{2} \frac{2}{\sqrt{\pi}} \int_{\delta_c/[\sqrt{2}\sigma_R(a)]}^{\infty} dx e^{-x^2} = \frac{1}{2} \mathrm{erfc}\left(\frac{\delta_c}{\sqrt{2}\sigma_R(a)}\right) ,$$

  where $\mathrm{erfc}(x)$ is the complementary error function.

The derivation of the halo mass function

- We assumed a Gaussian distribution for the probability of finding a filtered density contrast $\bar{\delta}(\boldsymbol{x})$ at $\boldsymbol{x}$:

$$p(\bar{\delta}, a) = \frac{1}{\sqrt{2\pi\sigma_R^2(a)}} \exp\left[-\frac{\bar{\delta}^2(\boldsymbol{x})}{2\sigma_R^2(a)}\right] ,$$

where the variance σ_R depends on time.

- The probability of finding the filtered density contrast at or above the linear density contrast for spherical collapse, $\bar{\delta} > \delta_c$, is equal to the fraction of the cosmic volume filled with haloes of mass M,

$$F(M, a) = \int_{\delta_c}^{\infty} \mathrm{d}\bar{\delta} p(\bar{\delta}, a) = \int_{\delta_c}^{\infty} \mathrm{d}\bar{\delta} \frac{1}{\sqrt{2\pi\sigma_R^2(a)}} \exp\left[-\frac{\bar{\delta}^2(\boldsymbol{x})}{2\sigma_R^2(a)}\right]$$

- After substitution, we obtain

$$F(M, a) = \frac{1}{2} \frac{2}{\sqrt{\pi}} \int_{\delta_c/[\sqrt{2}\sigma_R(a)]}^{\infty} \mathrm{d}x e^{-x^2} = \frac{1}{2} \mathrm{erfc}\left(\frac{\delta_c}{\sqrt{2}\sigma_R(a)}\right) ,$$

where $\mathrm{erfc}(x)$ is the complementary error function.

- This particular integral is named *complementary error function* because it also appears in cases where measurement values are Gaussian distributed.

Press-Schechter mass function

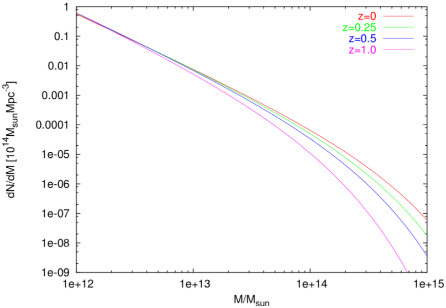

- For a power-law power spectrum with index n, $P_\delta(k) = Ak^n$, the Press-Schechter mass function is given by ($m = M/M_*$)

$$f(m,a)\mathrm{d}m \equiv \frac{\mathrm{d}N(m,a)}{\mathrm{d}m}\mathrm{d}m \propto m^{\alpha-2}\exp\left(-m^{2\alpha}\right)\mathrm{d}m,$$

where we defined $\alpha = 1/2 + n/6$ so that $\alpha = 0$ for $n = -3$.

- At small halo masses there is roughly an equal mass per log bin in halo mass,

$$m\,\mathrm{d}N/\mathrm{d}\log m = m^2\mathrm{d}N/\mathrm{d}m \approx \text{const.}$$

- At $z = 0$, $M_* = 1.3 \times 10^{14}\mathrm{M}_\odot$: the abundance of clusters is exponentially suppressed today and even more at early times (hierarchical structure formation!)

AIP

Halo formation as a random walk – 1

Progressive smoothing of the density field

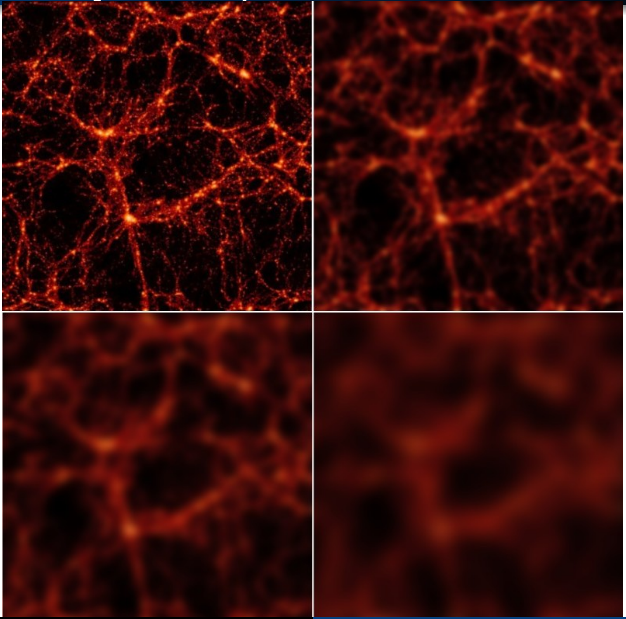

Halo formation as a random walk – 2

- Consider halo formation as a random walk $\Rightarrow$ correct normalisation of the Press-Schechter mass function

Halo formation as a random walk – 2

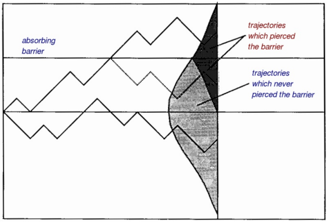

- Each trajectory shows the averaged density contrast $\bar{\delta}$ (on the y axis) versus decreasing radius R towards the right.
- They start at $\bar{\delta} = 0$ for very large radii (on the left) and may pierce the absorbing barrier at δ_c.
- The (Gaussian) probability distribtion of $\bar{\delta}$ is shown on the right.

- Consider halo formation as a random walk $\Rightarrow$ correct normalisation of the Press-Schechter mass function

Halo formation as a random walk – 2

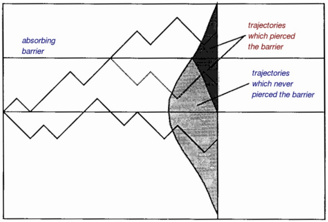

- Each trajectory shows the averaged density contrast $\bar{\delta}$ (on the *y* axis) versus decreasing radius *R* towards the right.
- They start at $\bar{\delta} = 0$ for very large radii (on the left) and may pierce the absorbing barrier at δ_c.
- The (Gaussian) probability distribtion of $\bar{\delta}$ is shown on the right.

- Consider halo formation as a random walk $\Rightarrow$ correct normalisation of the Press-Schechter mass function
- Given the density-contrast field δ, a large sphere is centered on some point $\boldsymbol{x}$ and its radius gradually shrunk. For each radius *R* of the sphere, the density contrast $\bar{\delta}$ averaged within *R* is measured and monitored as a function of *R*.

AIP

Halo formation as a random walk – 2

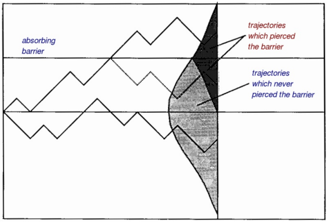

- Each trajectory shows the averaged density contrast $\bar{\delta}$ (on the y axis) versus decreasing radius R towards the right.
- They start at $\bar{\delta} = 0$ for very large radii (on the left) and may pierce the absorbing barrier at δ_{c}.
- The (Gaussian) probability distribtion of $\bar{\delta}$ is shown on the right.

- Consider halo formation as a random walk $\Rightarrow$ correct normalisation of the Press-Schechter mass function
- Given the density-contrast field δ, a large sphere is centered on some point $\boldsymbol{x}$ and its radius gradually shrunk. For each radius R of the sphere, the density contrast $\bar{\delta}$ averaged within R is measured and monitored as a function of R.
- By choosing a window function W_R whose Fourier transform has a sharp cut-off in k space, $\bar{\delta}$ will undergo a random walk because decreasing R corresponds to adding shells in k space which are independent of the modes which are already included.

AIP

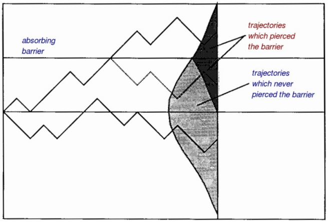

- Each trajectory shows the averaged density contrast $\bar{\delta}$ (on the y axis) versus decreasing radius R towards the right.
- They start at $\bar{\delta} = 0$ for very large radii (on the left) and may pierce the absorbing barrier at δ_c.
- The (Gaussian) probability distribtion of $\bar{\delta}$ is shown on the right.

- Consider halo formation as a random walk $\Rightarrow$ correct normalisation of the Press-Schechter mass function
- Given the density-contrast field δ, a large sphere is centered on some point $\boldsymbol{x}$ and its radius gradually shrunk. For each radius R of the sphere, the density contrast $\bar{\delta}$ averaged within R is measured and monitored as a function of R.
- By choosing a window function W_R whose Fourier transform has a sharp cut-off in k space, $\bar{\delta}$ will undergo a random walk because decreasing R corresponds to adding shells in k space which are independent of the modes which are already included.
- $\bar{\delta}(\boldsymbol{x})$ is thus following a random trajectory. A halo is expected to be formed at $\boldsymbol{x}$ if $\bar{\delta}(\boldsymbol{x})$ reaches δ_c for some radius R.
- If $\bar{\delta}(\boldsymbol{x}) < \delta_\mathrm{c}$ for some radius, it may well exceed δ_c for a smaller radius. Or, if $\bar{\delta}(\boldsymbol{x}) \geq \delta_\mathrm{c}$ for some radius, it may well drop below δ_c for a smaller radius.

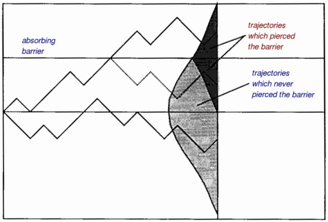

- Explain the physical reason for the missing factor of two and why this has been missed in the first derivation.

Halo formation as a random walk – 3

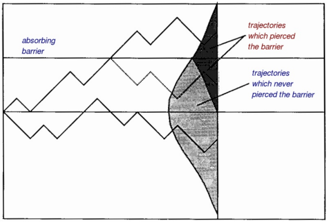

- Explain the physical reason for the missing factor of two and why this has been missed in the first derivation.
- We introduce an *absorbing barrier* at δ_c such that points $\boldsymbol{x}$ with trajectories $\bar{\delta}(\boldsymbol{x})$ vs. R which hit the barrier are removed from counting them as not being parts of halos. We follow the strategy of counting trajectories that do *not* make it into halos such that the complement of that union represent trajectories of halos.

Halo formation as a random walk – 3

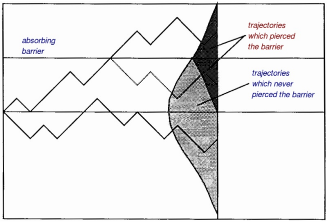

- Explain the physical reason for the missing factor of two and why this has been missed in the first derivation.
- We introduce an *absorbing barrier* at δ_c such that points $\boldsymbol{x}$ with trajectories $\bar{\delta}(\boldsymbol{x})$ vs. R which hit the barrier are removed from counting them as not being parts of halos. We follow the strategy of counting trajectories that do *not* make it into halos such that the complement of that union represent trajectories of halos.
- A trajectory meeting the boundary has equal probability for moving above or below. For any *forbidden* trajectory continuing above the boundary, there is an *allowed* mirror trajectory continuing below it, and conversely. For any trajectory reaching a point $\bar{\delta} < \delta_c$ exclusively along *allowed* trajectories, there is a path reaching its mirror point on the line $\bar{\delta} = \delta_c$ exclusively along *forbidden* trajectories, and conversely.

AIP

Halo formation as a random walk – 3

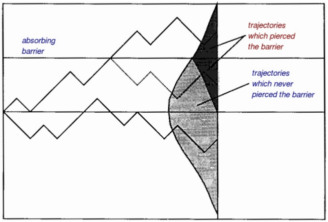

- Explain the physical reason for the missing factor of two and why this has been missed in the first derivation.
- We introduce an *absorbing barrier* at δ_c such that points $\boldsymbol{x}$ with trajectories $\bar{\delta}(\boldsymbol{x})$ vs. R which hit the barrier are removed from counting them as not being parts of halos. We follow the strategy of counting trajectories that do *not* make it into halos such that the complement of that union represent trajectories of halos.
- A trajectory meeting the boundary has equal probability for moving above or below. For any *forbidden* trajectory continuing above the boundary, there is an *allowed* mirror trajectory continuing below it, and conversely. For any trajectory reaching a point $\bar{\delta} < \delta_c$ exclusively along *allowed* trajectories, there is a path reaching its mirror point on the line $\bar{\delta} = \delta_c$ exclusively along *forbidden* trajectories, and conversely.
- Hence, the first derivation missed the dark grey halo population below the barrier that have pierced the barrier at some smoothing radius R.

Halo mass definitions

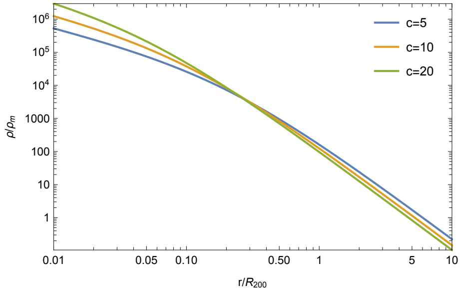

- The halo mass is Δ times the critical (mean) density times the halo volume,

$$M_\Delta = \Delta \rho_{\rm cr}(a) \left(\frac{4\pi}{3} r_\Delta^3\right) \quad \text{and} \quad M_{\Delta,\rm m} = \Delta \bar{\rho}_{\rm m}(a) \left(\frac{4\pi}{3} r_{\Delta,\rm m}^3\right)$$

where $\bar{\rho}_{\rm m}(a) = \rho_{\rm cr}(a)\Omega_{\rm m}(a)$.

Halo mass definitions

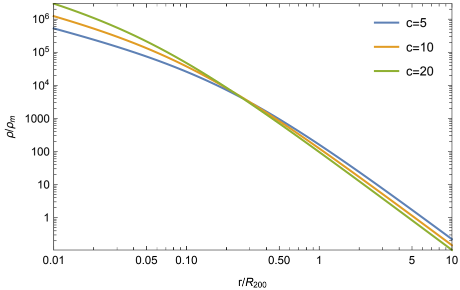

- The halo mass is Δ times the critical (mean) density times the halo volume,

$$M_\Delta = \Delta\rho_{\rm cr}(a)\left(\frac{4\pi}{3}r_\Delta^3\right) \quad \text{and} \quad M_{\Delta,\rm m} = \Delta\bar{\rho}_{\rm m}(a)\left(\frac{4\pi}{3}r_{\Delta,\rm m}^3\right)$$

where $\bar{\rho}_{\rm m}(a) = \rho_{\rm cr}(a)\Omega_{\rm m}(a)$.

- If we order the averaged density inside r_Δ ($r_{\Delta,\rm m}$) by increasing size:

$$200\rho_{\rm cr}\Omega_{\rm m} < 200\rho_{\rm cr} < 500\rho_{\rm cr}$$

then the corresponding virial radii and masses are ordered inversely because of the decreasing density profile:

$$M_{500} < M_{200} < M_{200\rm m}.$$

Orthonormal functions

- Plane waves form an orthonormal system on a homogeneous background? Does this mean that for small perturbations, waves are produced that are perpendicular to each other?

AIP

Orthonormal functions

- Plane waves form an orthonormal system on a homogeneous background? Does this mean that for small perturbations, waves are produced that are perpendicular to each other?$\Rightarrow$ no

- To understand the term *orthonormal system of functions*, first consider a 2D vector pointing to P, which can be decomposed into two unit vectors spanning the 2D plane: $\{\boldsymbol{e}_1, \boldsymbol{e}_2\}$ or $\{\boldsymbol{e}^1, \boldsymbol{e}^2\}$.
- If $\boldsymbol{e}^1 \perp \boldsymbol{e}^2$, we talk about an orthonormal basis system because the vector product vanishes if the vectors are not identical, $\boldsymbol{e}_i \cdot \boldsymbol{e}_j = \delta_{ij}$.

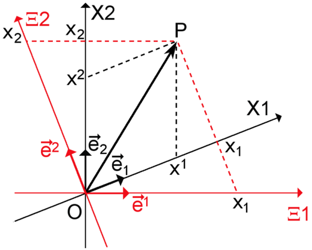

Orthonormal functions

- Plane waves form an orthonormal system on a homogeneous background? Does this mean that for small perturbations, waves are produced that are perpendicular to each other? $\Rightarrow$ no
- To understand the term *orthonormal system of functions*, first consider a 2D vector pointing to P, which can be decomposed into two unit vectors spanning the 2D plane: $\{\boldsymbol{e}_1, \boldsymbol{e}_2\}$ or $\{\boldsymbol{e}^1, \boldsymbol{e}^2\}$.
- If $\boldsymbol{e}^1 \perp \boldsymbol{e}^2$, we talk about an orthonormal basis system because the vector product vanishes if the vectors are not identical, $\boldsymbol{e}_i \cdot \boldsymbol{e}_j = \delta_{ij}$.

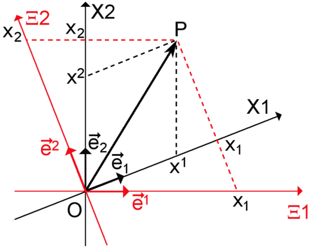

- The same idea applies to function space. The Fourier theorem states that you can decompose any smooth function $f(\boldsymbol{x})$ into plane waves

$$f(\boldsymbol{x}) = \int \frac{\mathrm{d}^3 k}{(2\pi)^3} \hat{f}(\boldsymbol{k}) \mathrm{e}^{-\mathrm{i}\boldsymbol{k}\cdot\boldsymbol{x}}$$

because these plane waves form an orthonormal system as you can see from taking the inner product of plane waves (defined via an integration over k space):

$$\delta_\mathrm{D}(\boldsymbol{x}-\boldsymbol{y}) = \int \frac{\mathrm{d}^3 k}{(2\pi)^3} \mathrm{e}^{-\mathrm{i}\boldsymbol{k}\cdot(\boldsymbol{x}-\boldsymbol{y})}.$$

Boussinesq approximation

- To first order, our conservation equations read

$$\frac{\partial \delta\rho}{\partial t} + \boldsymbol{\nabla}\cdot(\rho_0\delta\boldsymbol{v}) = 0, \tag{2}$$

$$\frac{\partial \delta\boldsymbol{v}}{\partial t} - \frac{\delta\rho}{\rho_0^2}\boldsymbol{\nabla}P_0 + \frac{\boldsymbol{\nabla}\delta P}{\rho_0} = 0, \tag{3}$$

$$\frac{1}{\gamma-1}\left(\frac{\partial \delta P}{\partial t} - \frac{\gamma k_{\mathrm{B}} T_0}{\bar{m}}\frac{\partial \delta\rho}{\partial t}\right) + \rho_0 T_0(\delta\boldsymbol{v}\cdot\boldsymbol{\nabla})s_0 = -\boldsymbol{\nabla}\cdot\delta\boldsymbol{Q}, \tag{4}$$

  where we have used $\boldsymbol{g} = \boldsymbol{\nabla}P_0/\rho_0$ in Eq. (3).
- In the Boussinesq approximation, we dropped the δP term in the energy equation (4) but not in momentum equation. Why?

AIP

Boussinesq approximation

- To first order, our conservation equations read

$$\frac{\partial \delta\rho}{\partial t} + \boldsymbol{\nabla}\cdot(\rho_0 \delta\boldsymbol{v}) = 0, \tag{2}$$

$$\frac{\partial \delta\boldsymbol{v}}{\partial t} - \frac{\delta\rho}{\rho_0^2}\boldsymbol{\nabla} P_0 + \frac{\boldsymbol{\nabla}\delta P}{\rho_0} = 0, \tag{3}$$

$$\frac{1}{\gamma-1}\left(\frac{\partial \delta P}{\partial t} - \frac{\gamma k_{\mathrm{B}} T_0}{\bar{m}}\frac{\partial \delta\rho}{\partial t}\right) + \rho_0 T_0 (\delta\boldsymbol{v}\cdot\boldsymbol{\nabla}) s_0 = -\boldsymbol{\nabla}\cdot\delta\boldsymbol{Q}, \tag{4}$$

  where we have used $\boldsymbol{g} = \boldsymbol{\nabla} P_0/\rho_0$ in Eq. (3).
- In the Boussinesq approximation, we dropped the δP term in the energy equation (4) but not in momentum equation. Why?
- Because the δP term in the momentum equation (3) is the only one providing the dynamics and advances $\delta\boldsymbol{v}$ in time, while there are the δP and $\delta\rho$ terms in the energy equation (4) of which the latter dominates in the Boussinesq approximation.

AIP

Generalized Rankine-Hugoniot conditions – 1

Show, that a Galilean transformation of the Rankine-Hugoniot shock jump conditions from the shock to the laboratory rest system leads to the generalized Rankine-Hugoniot conditions of mass, momentum, and energy conservation at a shock,

$$
\begin{aligned}
v_\mathrm{s}[\rho] &= [\rho u], && (5)\\
v_\mathrm{s}[\rho u] &= [\rho u^2 + P], && (6)\\
v_\mathrm{s}\left[\rho\frac{u^2}{2} + \varepsilon\right] &= \left[\left(\rho\frac{u^2}{2} + \varepsilon + P\right) u\right]. && (7)
\end{aligned}
$$

Here v_s and u denote the shock and the mean gas velocity measured in the laboratory rest system, $\varepsilon = \epsilon\rho$ is the thermal energy density, and we introduced the abbreviation $[F] = F_i - F_j$ for the jump of some quantity F across the shock.

Generalized Rankine-Hugoniot conditions – 1

Show, that a Galilean transformation of the Rankine-Hugoniot shock jump conditions from the shock to the laboratory rest system leads to the generalized Rankine-Hugoniot conditions of mass, momentum, and energy conservation at a shock,

$$\begin{aligned} v_\mathrm{s}[\rho] &= [\rho u], & (5)\\ v_\mathrm{s}[\rho u] &= [\rho u^2 + P], & (6)\\ v_\mathrm{s}\left[\rho\frac{u^2}{2} + \varepsilon\right] &= \left[\left(\rho\frac{u^2}{2} + \varepsilon + P\right)u\right]. & (7)\end{aligned}$$

Here v_s and u denote the shock and the mean gas velocity measured in the laboratory rest system, $\varepsilon = \epsilon\rho$ is the thermal energy density, and we introduced the abbreviation $[F] = F_i - F_j$ for the jump of some quantity F across the shock.

- Starting point: Rankine-Hugoniot jump conditions in the shock frame

$$\begin{aligned} [\rho v] &= 0,\\ \left[\rho v^2 + P\right] &= 0,\\ \left[E + \frac{P}{\rho}\right] &= 0 \qquad \text{where} \qquad E_i = \frac{1}{2}v_i^2 + \epsilon_i \end{aligned}$$

  denotes the specific total energy of region i (up-/downstream) in the shock frame and v_i is the velocity measured in the shock frame.

Generalized Rankine-Hugoniot conditions – 2

- We use the alternative formulation of the 3rd Rankine-Hugoniot condition

$$[v(\rho E + P)] = 0.$$

Generalized Rankine-Hugoniot conditions – 2

- We use the alternative formulation of the 3rd Rankine-Hugoniot condition

$$[v(\rho E + P)] = 0.$$

- Constancy of energy flux implies (using $v_i = u_i - v_s$ and $E_i = v_i^2/2 + \epsilon_i$)

$$
\begin{aligned}
0 = [v(\rho E + P)] &= \left[\left(\frac{1}{2}\rho v^2 + \rho\epsilon + P\right) v\right] \\
&= \left[\left(\frac{1}{2}\rho u^2 + \rho\epsilon - \rho u v_s + \frac{1}{2}\rho v_s^2 + P\right)(u - v_s)\right] \\
&= \left[\rho\tilde{E}u - \rho u^2 v_s + \frac{1}{2}\rho v_s^2 u + Pu - \left(\rho\tilde{E}v_s - \rho u v_s^2 + \frac{1}{2}\rho v_s^2 v_s + P v_s\right)\right] \\
&= \left[\rho\tilde{E}u - \rho u^2 v_s + \frac{1}{2}\rho v_s^2 u + Pu - \left(\rho\tilde{E}v_s - \rho u v_s^2 + \frac{1}{2}\rho v_s^2 v_s + P v_s\right)\right] \\
&= [(\rho\tilde{E} + P)u] - v_s[\rho\tilde{E}] - v_s\left(\left[\rho u^2 + P\right] - v_s[\rho u]\right) + \frac{1}{2}v_s^2\left([\rho u] - v_s[\rho]\right) \\
&= [(\rho\tilde{E} + P)u] - v_s[\rho\tilde{E}]
\end{aligned}
$$

where $\tilde{E}_i = u_i^2/2 + \epsilon_i$ and we used Eqs. (5) and (6) in the last step.

AIP

Sloshing cool core after a cluster merger: IDCS 1426

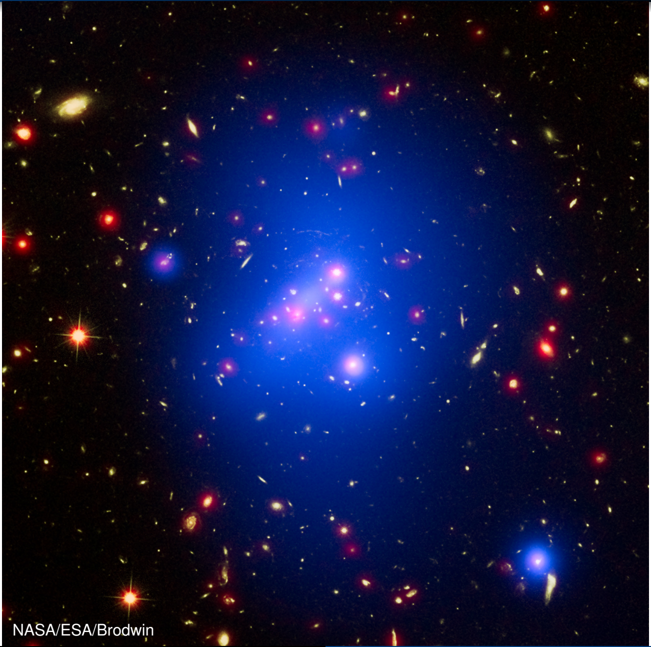

Distant lensed galaxy in galaxy cluster Abell 2744

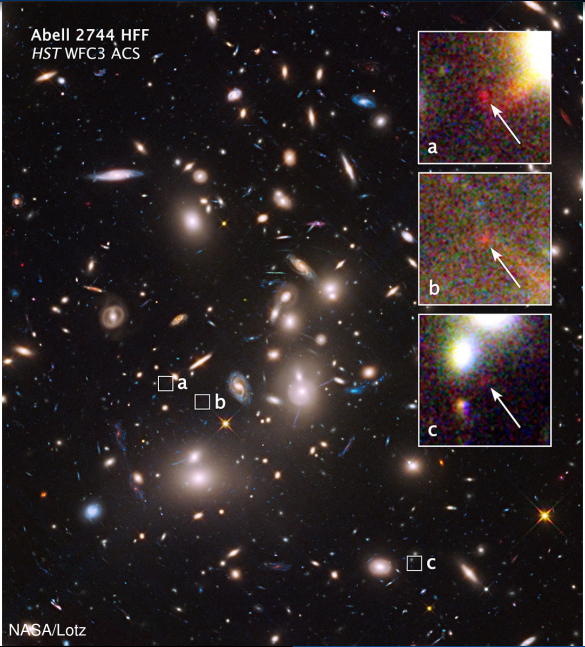

Distant and ancient: the galaxy cluster SPT 0615

One of the most massive galaxy clusters: RCS2 J2327

One of the most massive galaxy clusters: RCS2 J2327

Star formation in lensed galaxy in cluster SDSS 1110

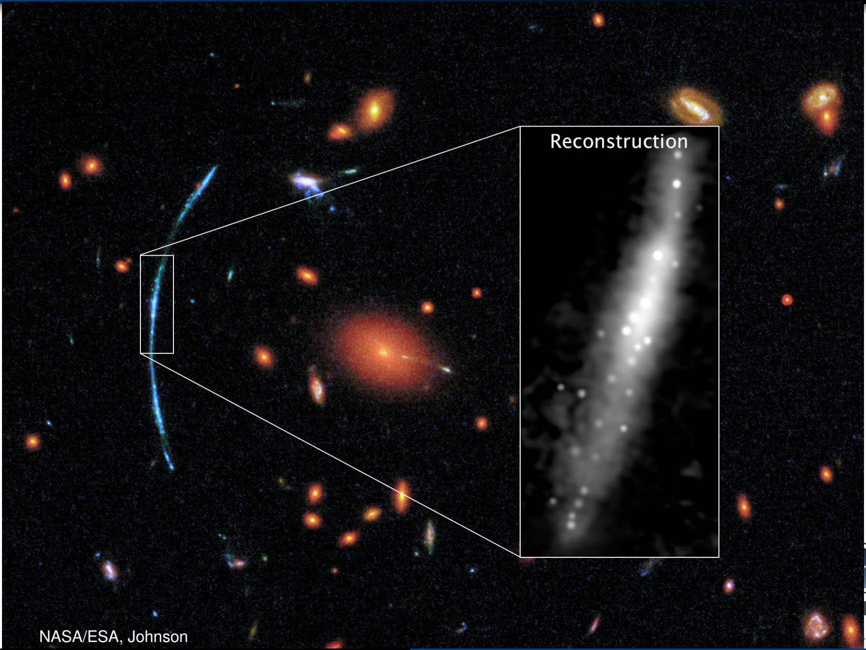

“Smiley” image: Einstein ring in cluster SDSS 1038

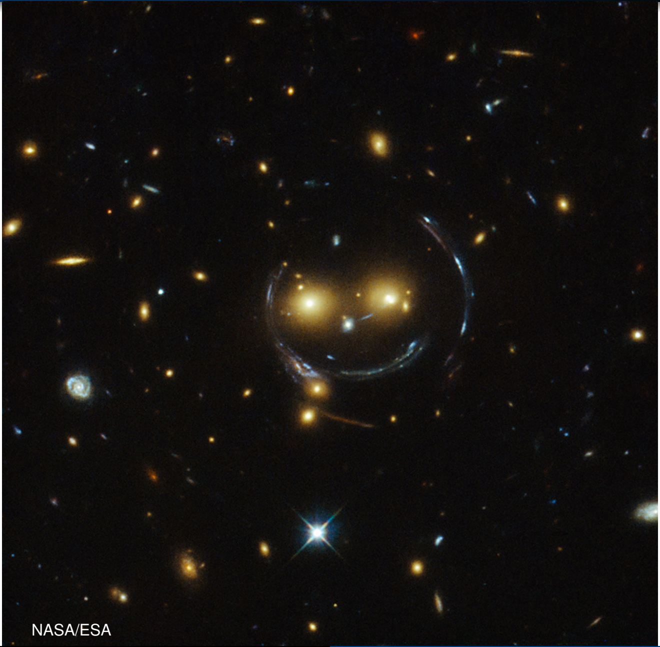

A menagerie of galaxies – the cluster ACO S 295

MACS 0138 – cosmic lens flare

MACS 0138 – detecting distant supernovae

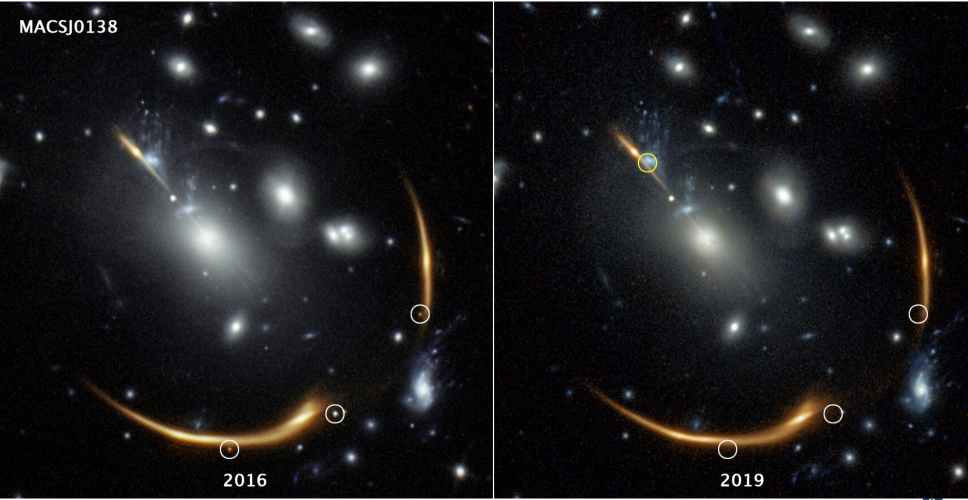

NASA/ESA, Rodney, Brammer, DePasquale

ICM turbulence in Perseus and Virgo (X-rays)

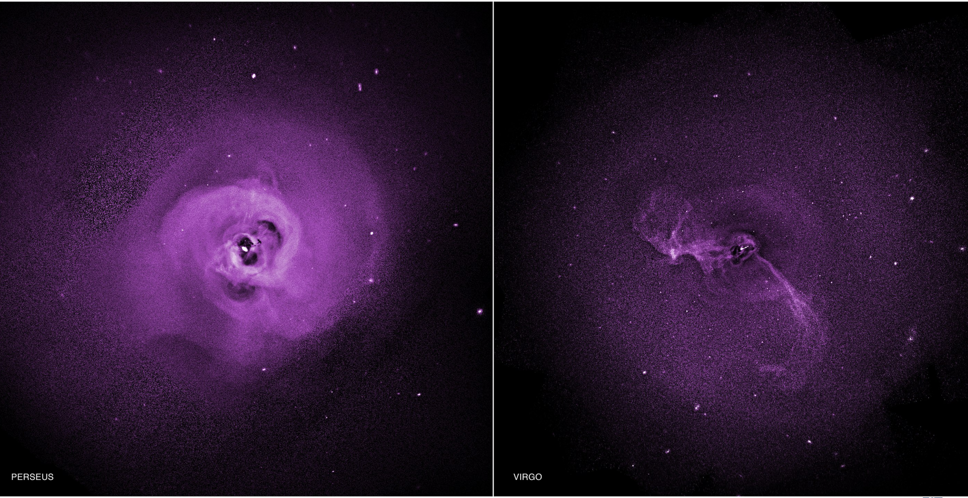

NASA/CXC, Zhuravleva

Summary of the tutorial:

- putting galaxy clusters into historical context
- going beyond clusters: the existence of superclusters
- putting the lectures into context
- answering your questions in the order of the lectures
- visual impressions: from images to astrophysics